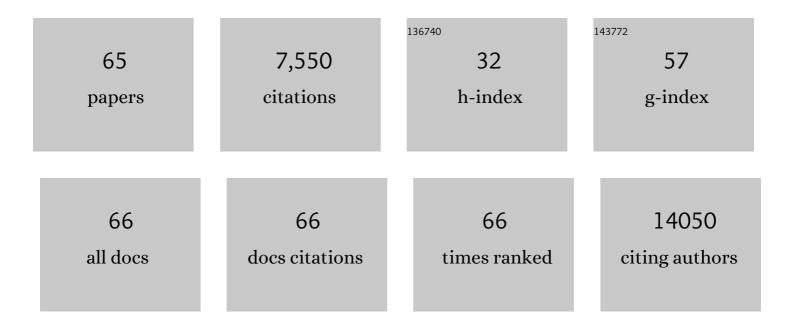
List of Publications by Year in descending order

Source: https://exaly.com/author-pdf/53493/publications.pdf Version: 2024-02-01



#	Article	IF	CITATIONS
1	The PET tracer [¹¹ C]MK-6884 quantifies M4 muscarinic receptor in rhesus monkeys and patients with Alzheimer's disease. Science Translational Medicine, 2022, 14, eabg3684.	5.8	10
2	PET/CT Imaging of 89Zr-N-sucDf-Pembrolizumab in Healthy Cynomolgus Monkeys. Molecular Imaging and Biology, 2021, 23, 250-259.	1.3	18
3	High Availability of the α7-Nicotinic Acetylcholine Receptor in Brains of Individuals with Mild Cognitive Impairment: A Pilot Study Using ¹⁸ F-ASEM PET. Journal of Nuclear Medicine, 2020, 61, 423-426.	2.8	22
4	Development of a high-resolution and high-efficiency single-photon detector for studying cardiovascular diseases in mice. European Physical Journal Plus, 2020, 135, 1.	1.2	0
5	Enhancement of Radiotherapy with Human Mesenchymal Stem Cells Containing Gold Nanoparticles. Tomography, 2020, 6, 373-378.	0.8	4
6	PET imaging of microglia by targeting macrophage colony-stimulating factor 1 receptor (CSF1R). Proceedings of the National Academy of Sciences of the United States of America, 2019, 116, 1686-1691.	3.3	140
7	Positron Emission Tomography Studies of the Glial Cell Marker Translocator Protein in Patients With Psychosis: A Meta-analysis Using Individual Participant Data. Biological Psychiatry, 2018, 84, 433-442.	0.7	103
8	Desmin Phosphorylation Triggers Preamyloid Oligomers Formation and Myocyte Dysfunction in Acquired Heart Failure. Circulation Research, 2018, 122, e75-e83.	2.0	46
9	¹⁸ F-XTRA PET for Enhanced Imaging of the Extrathalamic α4β2 Nicotinic Acetylcholine Receptor. Journal of Nuclear Medicine, 2018, 59, 1603-1608.	2.8	15
10	Translational evaluation of translocator protein as a marker of neuroinflammation in schizophrenia. Molecular Psychiatry, 2018, 23, 323-334.	4.1	159
11	The distribution of the alpha7 nicotinic acetylcholine receptor in healthy aging: An in vivo positron emission tomography study with [18F]ASEM. NeuroImage, 2018, 165, 118-124.	2.1	27
12	Imaging of Glial Cell Activation and White Matter Integrity in Brains of Active and Recently Retired National Football League Players. JAMA Neurology, 2017, 74, 67.	4.5	134
13	A PSMA-targeted theranostic agent for photodynamic therapy. Journal of Photochemistry and Photobiology B: Biology, 2017, 167, 111-116.	1.7	39
14	MR-Guided Delivery of Hydrophilic Molecular Imaging Agents Across the Blood-Brain Barrier Through Focused Ultrasound. Molecular Imaging and Biology, 2017, 19, 24-30.	1.3	15
15	Neuroimaging of translocator protein in patients with systemic lupus erythematosus: a pilot study using [¹¹ C]DPA-713 positron emission tomography. Lupus, 2017, 26, 170-178.	0.8	25
16	In vivo markers of inflammatory response in recent-onset schizophrenia: a combined study using [11C]DPA-713 PET and analysis of CSF and plasma. Translational Psychiatry, 2016, 6, e777-e777.	2.4	134
17	18F-FNDP for PET Imaging of Soluble Epoxide Hydrolase. Journal of Nuclear Medicine, 2016, 57, 1817-1822.	2.8	19
18	Development of a High-Affinity PET Radioligand for Imaging Cannabinoid Subtype 2 Receptor. Journal of Medicinal Chemistry, 2016, 59, 7840-7855.	2.9	47

#	Article	IF	CITATIONS
19	[¹⁸ F]Fluoroethyl Triazole Substituted PSMA Inhibitor Exhibiting Rapid Normal Organ Clearance. Bioconjugate Chemistry, 2016, 27, 1655-1662.	1.8	15
20	[¹⁸ F]Fluorobenzoyllysinepentanedioic Acid Carbamates: New Scaffolds for Positron Emission Tomography (PET) Imaging of Prostate-Specific Membrane Antigen (PSMA). Journal of Medicinal Chemistry, 2016, 59, 206-218.	2.9	37
21	[64Cu]XYIMSR-06: A dual-motif CAIX ligand for PET imaging of clear cell renal cell carcinoma. Oncotarget, 2016, 7, 56471-56479.	0.8	49
22	Cannabinoid CB2 Receptors in a Mouse Model of AÎ ² Amyloidosis: Immunohistochemical Analysis and Suitability as a PET Biomarker of Neuroinflammation. PLoS ONE, 2015, 10, e0129618.	1.1	83
23	Evaluation of a PSMA-targeted BNF nanoparticle construct. Nanoscale, 2015, 7, 4432-4442.	2.8	35
24	18F-FDG-PET/CT Imaging of Drug-Induced Metabolic Changes in Genetically Engineered Mouse Lung Cancer Models. Cold Spring Harbor Protocols, 2015, 2015, pdb.prot078246.	0.2	4
25	Noninvasive Imaging of Tumor Burden and Molecular Pathways in Mouse Models of Cancer. Cold Spring Harbor Protocols, 2015, 2015, pdb.top069930.	0.2	28
26	Preclinical Evaluation of 86Y-Labeled Inhibitors of Prostate-Specific Membrane Antigen for Dosimetry Estimates. Journal of Nuclear Medicine, 2015, 56, 628-634.	2.8	35
27	Neuroinflammation and brain atrophy in former NFL players: An in vivo multimodal imaging pilot study. Neurobiology of Disease, 2015, 74, 58-65.	2.1	208
28	Regional brain distribution of translocator protein using [11C]DPA-713 PET in individuals infected with HIV. Journal of NeuroVirology, 2014, 20, 219-232.	1.0	78
29	Co-Clinical Trials Demonstrate Superiority of Crizotinib to Chemotherapy in <i>ALK</i> -Rearranged Non–Small Cell Lung Cancer and Predict Strategies to Overcome Resistance. Clinical Cancer Research, 2014, 20, 1204-1211.	3.2	57
30	AEC-1 Promoter–Mediated Imaging of Prostate Cancer. Cancer Research, 2014, 74, 5772-5781.	0.4	33
31	¹⁸ F-ASEM, a Radiolabeled Antagonist for Imaging the α7-Nicotinic Acetylcholine Receptor with PET. Journal of Nuclear Medicine, 2014, 55, 672-677.	2.8	65
32	Targeted Imaging of Ewing Sarcoma in Preclinical Models Using a 64Cu-Labeled Anti-CD99 Antibody. Clinical Cancer Research, 2014, 20, 678-687.	3.2	23
33	Evaluation of Prostate-Specific Membrane Antigen as an Imaging Reporter. Journal of Nuclear Medicine, 2014, 55, 805-811.	2.8	38
34	Antiproliferative Effects of CDK4/6 Inhibition in <i>CDK4</i> -Amplified Human Liposarcoma <i>In Vitro</i> and <i>In Vivo</i> . Molecular Cancer Therapeutics, 2014, 13, 2184-2193.	1.9	102
35	Radiochemical synthesis and in vivo evaluation of [18F]AZ11637326: An agonist probe for the α7 nicotinic acetylcholine receptor. Nuclear Medicine and Biology, 2013, 40, 731-739.	0.3	18
36	Characterization of Torin2, an ATP-Competitive Inhibitor of mTOR, ATM, and ATR. Cancer Research, 2013, 73, 2574-2586.	0.4	170

#	Article	IF	CITATIONS
37	Incongruity of Imaging Using Fluorescent 2-DG Conjugates Compared to 18F-FDG in Preclinical Cancer Models. Molecular Imaging and Biology, 2012, 14, 553-560.	1.3	25
38	A murine lung cancer co-clinical trial identifies genetic modifiers of therapeutic response. Nature, 2012, 483, 613-617.	13.7	430
39	Evaluation of a Multi-pinhole Collimator for Imaging Small Animals with Different Sizes. Molecular Imaging and Biology, 2012, 14, 60-69.	1.3	20
40	Development and Validation of a Monte Carlo Simulation Tool for Multi-Pinhole SPECT. Molecular Imaging and Biology, 2010, 12, 295-304.	1.3	15
41	Selective inhibition of BET bromodomains. Nature, 2010, 468, 1067-1073.	13.7	3,456
42	Inhibition of ALK, PI3K/MEK, and HSP90 in Murine Lung Adenocarcinoma Induced by <i>EML4-ALK</i> Fusion Oncogene. Cancer Research, 2010, 70, 9827-9836.	0.4	181
43	Toward Quantitative Small Animal Pinhole SPECT: Assessment of Quantitation Accuracy Prior to Image Compensations. Molecular Imaging and Biology, 2009, 11, 195-203.	1.3	28
44	Quantification of the Multiplexing Effects in Multi-Pinhole Small Animal SPECT: A Simulation Study. IEEE Transactions on Nuclear Science, 2009, 56, 2636-2643.	1.2	50
45	An Immunotolerant HER-2/ <i>neu</i> Transgenic Mouse Model of Metastatic Breast Cancer. Clinical Cancer Research, 2008, 14, 6116-6124.	3.2	24
46	X-ray fluorescence study with pixellated CZT radiation sensors. , 2008, , .		4
47	Integration of SimSET photon history generator in GATE for efficient Monte Carlo simulations of pinhole SPECT. Medical Physics, 2008, 35, 3278-3284.	1.6	24
48	Detection of Dose Response in Chronic Doxorubicin-Mediated Cell Death with Cardiac Technetium 99m Annexin V Single-Photon Emission Computed Tomography. Molecular Imaging, 2008, 7, 7290.2008.00015.	0.7	36
49	Detection of dose response in chronic doxorubicin-mediated cell death with cardiac technetium 99m annexin V single-photon emission computed tomography. Molecular Imaging, 2008, 7, 132-8.	0.7	19
50	Development of simulation tools for small animal SPECT/MRI reconstruction study. , 2007, , .		2
51	Pinhole SPECT With Different Data Acquisition Geometries: Usefulness of Unified Projection Operators in Homogeneous Coordinates. IEEE Transactions on Medical Imaging, 2007, 26, 298-308.	5.4	45
52	Quantitative Rotating Multisegment Slant-Hole SPECT Mammography With Attenuation and Collimator-Detector Response Compensation. IEEE Transactions on Medical Imaging, 2007, 26, 906-916.	5.4	14
53	Performance evaluation of the GE healthcare eXplore VISTA dual-ring small-animal PET scanner. Journal of Nuclear Medicine, 2006, 47, 1891-900.	2.8	167
54	High-resolution molecular imaging techniques for cardiovascular research. Journal of Nuclear Cardiology, 2005, 12, 261-267.	1.4	9

#	Article	IF	CITATIONS
55	Imaging bacterial infections with radiolabeled 1-(2'-deoxy-2'-fluoro-Â-D-arabinofuranosyl)-5-iodouracil. Proceedings of the National Academy of Sciences of the United States of America, 2005, 102, 1145-1150.	3.3	125
56	Radiolabeled Small-Molecule Ligands for Prostate-Specific Membrane Antigen: In vivo Imaging in Experimental Models of Prostate Cancer. Clinical Cancer Research, 2005, 11, 4022-4028.	3.2	246
57	Advanced cancers: eradication in all cases using 3-bromopyruvate therapy to deplete ATP. Biochemical and Biophysical Research Communications, 2004, 324, 269-275.	1.0	331
58	Evaluation of rotating slant-hole SPECT mammography using Monte Carlo simulation methods. IEEE Transactions on Nuclear Science, 2003, 50, 105-109.	1.2	15
59	Performance evaluation of A-SPECT: a high resolution desktop pinhole SPECT system for imaging small animals. IEEE Transactions on Nuclear Science, 2002, 49, 2139-2147.	1.2	134
60	Pinhole SPECT of mice using the LumaGEM gamma camera. IEEE Transactions on Nuclear Science, 2001, 48, 830-836.	1.2	90
61	Evaluation of A-SPECT: a desktop pinhole SPECT system for small animal imaging. , 0, , .		10
62	Optimal camera placement for cardiac imaging using rotating multi-segment slant-hole single photon emission computed tomography. , 0, , .		0
63	Implementation of short-scan reconstruction with compensation for geometric alignment for a microCT system. , 0, , .		0
64	Evaluation of rotating slant hole SPECT mammography with respect to planar scintimammography using Monte Carlo simulation methods. , 0, , .		5
65	Design of a Novel Pinhole Collimator System for SPECT Imaging of Small Animals with Different Sizes. , 0, , .		7